Distributed Blowing and Suction for the Purpose of Streak Control in a Boundary Layer Subjected to a Favorable Pressure Gradient

Eric Forgoston[*] and Anatoli Tumin[†]

The University of Arizona, Tucson, Arizona 85721

David E. Ashpis[‡]

NASA Glenn Research Center at Lewis Field, Cleveland, Ohio 44135

An analysis of the optimal control by blowing and suction in order to generate streamwise velocity streaks is presented. The problem is examined using an iterative process that employs the Parabolized Stability Equations for an incompressible fluid along with its adjoint equations. In particular, distributions of blowing and suction are computed for both the normal and tangential velocity perturbations for various choices of parameters.

Nomenclature

E	energy norm
G	energy growth ratio
L_{ref}	reference length
p	pressure disturbance
U	mean-flow streamwise velocity
U_{ref}	reference velocity
u	streamwise velocity disturbance
V	mean-flow normal velocity
V_w	normal velocity of blowing or suction at the wall
v	normal velocity disturbance
W_w	tangential velocity of blowing or suction at the wall
w	spanwise velocity disturbance
β	spanwise wave number
ϵ	$\sqrt{\nu/U_{ref}L_{ref}}$
ν	kinematic viscosity
ρ	density

Superscript
T	transpose

[*]Graduate Student, Program in Applied Mathematics. Member AIAA.
[†]Associate Professor, Department of Aerospace and Mechanical Engineering. Senior Member AIAA.
[‡]Aerospace Engineer. Senior Member AIAA.

American Institute of Aeronautics and Astronautics

Subscript
exit exit conditions
in   start point
out   end point
ref   reference
x $\partial/\partial x$
y $\partial/\partial y$

I.   Introduction

The performance of low-pressure turbines (LPT's) is strongly affected by flow separation. There is a possibility of delaying the boundary layer separation by tripping the boundary layer with the use of generators placed on the surface of the airfoil. Usually, a trial-and-error method is used to determine an appropriate placement of the control elements. However, this approach is time consuming and expensive.

One of the possible scenarios of early transition is associated with the development of velocity streaks. Due to a secondary instability mechanism (associated with the presence of free stream turbulence), velocity streaks in the boundary layer flow may lead to bypass transition at low Reynolds numbers. This earlier transition to turbulence can prevent the flow separation. To generate the streaks, one may introduce a system of counter-rotating streamwise vortices that decay downstream and result in a streaky structure in the boundary layer.

Analysis of optimal streamwise vortices within the scope of the transient growth theory[1] indicated that a favorable pressure gradient suppresses the transient growth mechanism. Therefore, a row of localized generators placed on the wall will be unlikely to generate the optimal perturbation. However, there is also a possibility that the same streaky structures can be generated with the help of distributed generators.

In Ref. 2, a model of optimal control of the algebraically growing perturbations by blowing and suction at the wall was proposed. The model provided a tool to find the distribution of blowing and suction at the wall that suppresses the streaky structures. Because the theoretical model[2] is based on linearized equations, it can also be used to optimize the distributed generators in order to generate the streaky structures equivalent to those generated by the optimal perturbation.

In the present work, the distributed generators are emulated by the normal and tangential velocity perturbations at the wall. A parametric study of these generators has been performed for a flat plate without a pressure gradient and for a flat plate with a favorable pressure gradient.

II.   Governing Equations

We consider steady three-dimensional disturbances in an incompressible two-dimensional boundary layer. The streamwise coordinate, x, is made nondimensional using a reference length scale L_{ref}, while the normal and spanwise coordinates, y and z respectively, are made nondimensional using the length scale $\sqrt{\nu L_{ref}/U_{ref}}$, where ν is viscosity and U_{ref} is a reference velocity. With the help of a small parameter ϵ defined as $\epsilon = \sqrt{\nu/U_{ref}L_{ref}}$, the following scalings are assumed for the streamwise, normal and spanwise velocity disturbances, u, v and w respectively, and the pressure disturbance, p:

$$u \sim U_{ref}, \quad v \sim \epsilon U_{ref}, \quad w \sim \epsilon U_{ref}, \quad p \sim \epsilon^2 \rho U_{ref} \tag{1}$$

This choice of scaling of the linearized Navier-Stokes equations along with the neglect of curvature effects leads to the governing equations for Görtler instability with Görtler number $G = 0$. The solution is assumed to be periodic in the spanwise direction z. It is therefore possible to assume solutions of the form $u = u(x,y)\cos\beta z$, $v = v(x,y)\cos\beta z$, $w = w(x,y)\sin\beta z$ and $p = p(x,y)\cos\beta z$ where β is the spanwise wave number. The

American Institute of Aeronautics and Astronautics

governing equations are given in dimensionless form as:

$$u_x + v_y + \beta w = 0 \tag{2}$$

$$(Uu)_x + Vu_y + vU_y = u_{yy} - \beta^2 u \tag{3}$$

$$(uV + vU)_x + (2Vv)_y + \beta V w + p_y = v_{yy} - \beta^2 v \tag{4}$$

$$(Uw)_x + (Vw)_y - \beta p = w_{yy} - \beta^2 w \tag{5}$$

where $U(x,y)$ is the mean-flow streamwise velocity and $V(x,y)$ is the mean-flow normal velocity. U is scaled with U_{ref} and V is scaled with ϵU_{ref}.

Since we investigate two types of distributed generators, there are two sets of boundary conditions. The first set of boundary conditions is associated with the normal velocity perturbation and is given as:

$$y = 0: \quad u = w = 0, \; v = V_w \quad \text{and} \quad y \to \infty: \quad u, w, p = 0 \tag{6}$$

where V_w is the normal velocity of blowing or suction at the wall ($y = 0$). The second set of boundary conditions is associated with the tangential velocity perturbation and is given as:

$$y = 0: \quad u = v = 0, \; w = W_w \quad \text{and} \quad y \to \infty: \quad u, w, p = 0 \tag{7}$$

where W_w is the tangential velocity of blowing or suction at the wall. The system of equations (2-5) can be solved subject to the boundary conditions (6) or (7) with a prescribed initial velocity perturbation at $x = x_0$.

Introducing the vector $\mathbf{f} = (u, v, w, p)^T$, where the superscript "T" means transpose, the governing equations (2-5) can be recast as

$$(\mathbf{Af})_x = \mathbf{B}_0 \mathbf{f} + \mathbf{B}_1 \mathbf{f}_y + \mathbf{B}_2 \mathbf{f}_{yy} \tag{8}$$

where $\mathbf{A}$, $\mathbf{B}_0$, $\mathbf{B}_1$, and $\mathbf{B}_2$ are 4×4 matrices given in the appendix as well as in Ref. 1 and Ref. 3.

III. Optimal Control: Model

A. Model

We are interested in computing the distribution of blowing and suction that can generate a streamwise velocity streak equivalent to that which will be generated by an initial optimal perturbation. Since the problem is linear, this distribution can be determined using the optimal control model of Cathalifaud and Luchini.[2]

Given an optimal initial disturbance at x_0, the method determines a control by blowing and suction that suppresses the streamwise streaks. The method of optimal control is based on the minimization of an objective functional subject to constraints. Using standard mathematical techniques from control theory,[4] a system of differential equations (direct and adjoint problems) along with conditions of optimality is formulated. The solution gives the optimal control and is computed using an iterative procedure.

For the sake of clarity, we recapitulate the formulation of the optimal control model. In this problem, $\mathbf{f}$ is the vector containing the state variables, V_w (or W_w) is the control variable and the constraints are given by the direct problem (Eq. 8) along with its boundary conditions and initial condition. Additionally, $\boldsymbol{\xi} = (a, b, c, d)^T$ is the vector containing the Lagrange multipliers and ζ is the Lagrange multiplier associated with the wall receptivity. Although we continue the model description using the control variable V_w, the model is valid for W_w as well. The objective functional to be minimized is given as

$$\mathcal{J}(\mathbf{f}, V_w) = \frac{1}{2} \int_0^\infty u^2(x_{out}, y) \; dy \tag{9}$$

American Institute of Aeronautics and Astronautics

Minimization of this functional is equivalent to minimizing the energy of the disturbance at the output cross-section. Note that this objective functional does not take the "cost" of the control into account.

The Lagrangian functional is defined as

$$\mathcal{L}(\mathbf{f}, V_w, \boldsymbol{\xi}, \zeta) = \mathcal{J}(\mathbf{f}, V_w) - \int_{x_{in}}^{x_{out}} \int_0^\infty \boldsymbol{\xi} \cdot [(\mathbf{A}\mathbf{f})_x - \mathbf{B}_0\mathbf{f} - \mathbf{B}_1\mathbf{f}_y - \mathbf{B}_2\mathbf{f}_{yy}] \, dy \, dx - \int_{x_{in}}^{x_{out}} \zeta(x) \cdot (v(x,o) - V_w(x)) \, dx \tag{10}$$

and the equations of the adjoint problem can be found from the condition of extremality

$$\delta\mathcal{L}_{\mathbf{f}} = \lim_{\tau \to 0} \frac{\mathcal{L}(\mathbf{f} + \tau\delta\mathbf{f}, V_w, \boldsymbol{\xi}, \zeta) - \mathcal{L}(\mathbf{f}, V_w, \boldsymbol{\xi}, \zeta)}{\tau} = 0 \tag{11}$$

where $\delta\mathbf{f}$ is a variation of $\mathbf{f}$. The equations for the adjoint problem are

$$a_x + Ub_x + Vc_x + (Vb)_y + b_{yy} - \beta^2 b = 0 \tag{12}$$

$$Uc_x + 2Vc_y + c_{yy} - \beta^2 c - U_y b + a_y = 0 \tag{13}$$

$$ud_x + Vd_y + d_{yy} - \beta^2 d - \beta(a + Vc) = 0 \tag{14}$$

$$c_y + \beta d = 0 \tag{15}$$

The boundary conditions are

$$y = 0: \quad a = b = c = 0 \quad \text{and} \quad y \to \infty: \quad a + c_y + 2cV = 0 \tag{16}$$

and the initial condition of the adjoint equations, $u_a(x_{out}, y)$ is given by the solution to the direct problem at the end point, $u(x_{out}, y)$. Furthermore, the optimality condition is given by

$$y = 0: \quad a + c_y = 0 \tag{17}$$

B. Iterative Procedure

An iterative procedure is used to numerically determine the optimal control. The algorithm is given as:

1. The forward problem using the direct equations is solved from $x = x_{in}$ to $x = x_{out}$ subject to the boundary conditions and the initial condition (the optimal perturbation).

2. The objective functional is computed at the end of the forward iteration, and it is compared to the value of the objective functional found at the end of the first iteration. If the ratio is less than a prescribed value, the iterations stop. Otherwise, the initial condition for the backward problem is found from the solution to the forward problem at $x = x_{out}$.

3. The backward problem using the adjoint equations is solved from $x = x_{out}$ to $x = x_{in}$ subject to the boundary conditions and the initial condition for the adjoint problem.

4. A new initial condition and a new boundary condition for V_w is computed, and the forward problem is iterated. The loop continues until the optimization is considered to have converged.

Given an initial optimal perturbation, this iterative scheme determines the optimal control by blowing and suction to suppress the streamwise velocity streak that would have been generated by the initial disturbance (if there was no control). Again, since the problem is linear, this same optimal control by blowing and suction can be used to generate this same velocity streak in the case of zero initial disturbance.

IV. Results

A. Flat Plate Without a Pressure Gradient

We consider a flat plate of length L in a flow having free stream velocity U_∞. Therefore, this case has the scalings $L_{ref} = L$ and $U_{ref} = U_\infty$. The flow control area is distributed over the interval $[x_0, 1]$, where x_0, the location of the optimal inflow disturbance, is varied. For each pair of the parameters β and x_0, a transiently growing optimal inflow was determined using the model described by Andersson, et.al.,[3] Luchini[5] and Tumin, et.al.[1]

The optimal inflow disturbance is found in terms of the energy growth ratio $G = E_{out}/E_{in}$, where E_{in} is an input energy norm and E_{out} is an output energy norm. Employing the fact that the optimal disturbances at the input are represented by streamwise vortices with corresponding streamwise streaks at the output, we use the following energy norms of Ref. 1 and Ref. 5:

$$E_{in} = \epsilon^2 \int_0^{y_{max}} (v^2 + w^2)\, dy \quad \text{and} \quad E_{out} = \int_0^{y_{max}} u^2\, dy \qquad (18)$$

As an example, the streamwise velocity perturbation at $x = 1.0$ is shown for $\beta = 0.4$ and $x_0 = 0.25$ in Fig. 1. Figure 2 shows the optimal velocity perturbations at $x_0 = 0.25$ that corresponds to the streamwise velocity perturbation at $x = 1.0$ shown in Fig. 1.
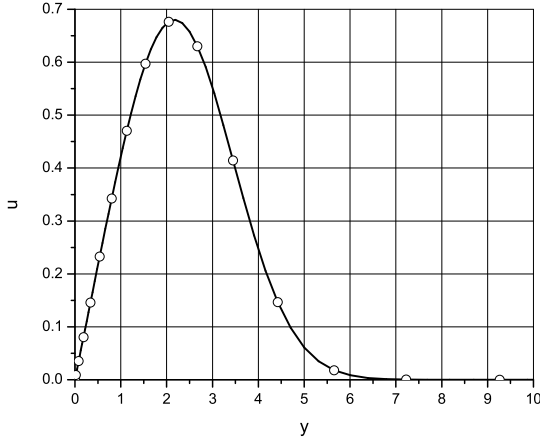

Figure 1. Streamwise velocity perturbation at $x = 1.0$ for $\beta = 0.4$ and $x_0 = 0.25$.
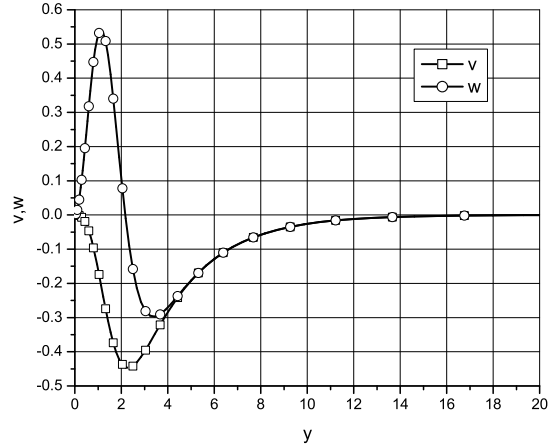
Figure 2. Optimal velocity perturbations for $\beta = 0.4$ at $x_0 = 0.25$ corresponding to the streamwise velocity perturbation at $x = 1.0$ shown in Fig. 1.

After the optimal inflow was computed, the iterative procedure described in Section III was applied to calculate the wall velocity distribution that would suppress the velocity streaks at $x = 1.0$. Due to the linear character of the problem, this velocity distribution is also the optimal distribution for the generation of a streamwise velocity streak that has the same properties as in the case of an optimal inflow perturbation.

Figures 3 - 6 depict the blowing and suction distribution of V_w, the normal velocity at the wall, that will lead to optimal streaky structures for various combinations of the parameters β and x_0. Figure 3 shows V_w for $x_0 = 0.1$ for four choices of β ($\beta = 0.2, 0.4, 0.6$ and 0.8). For these four values of β, Fig. 4 shows V_w for $x_0 = 0.25$, Fig. 5 shows V_w for $x_0 = 0.4$ and Fig. 6 shows V_w for $x_0 = 0.55$.

In each figure, one can see that for optimal control, a large region of blowing exists at the start of the flow control interval. For each choice of x_0, the magnitude of V_w at x_0 increases as β increases. Also, for

American Institute of Aeronautics and Astronautics

each choice of β, the magnitude of V_w at x_0 increases as x_0 increases. After the interval of blowing, there is a region of suction. The location of this blowing-suction transition within the flow control interval remains roughly the same for a choice of β. Within this region of suction, the maximum magnitude of V_w is associated with the largest value of β for a given x_0; also, this magnitude increases as x_0 increases. Beyond this region of suction there are alternating smaller regions of blowing and suction. The number of these regions increases as x_0 increases. Furthermore, because of the scalings, the physical size of V_w is very small.

Figures 7 - 10 depict the blowing and suction distribution of W_w, the tangential velocity at the wall, that will lead to optimal streaky structures for various combinations of the parameters β and x_0. Figure 7 shows W_w for $x_0 = 0.1$ for four choices of β ($\beta = 0.2$, 0.4, 0.6 and 0.8). For these four values of β, Fig. 8 shows W_w for $x_0 = 0.25$, Fig. 9 shows W_w for $x_0 = 0.4$ and Fig. 10 shows W_w for $x_0 = 0.55$.

Statements similar to those made about Figs. 3 - 6 can be written regarding the relative magnitudes of W_w for fixed values of x_0 and β. One major difference is that the first region in the flow control interval is one of suction. This region is followed by a region of blowing, and then there are alternating regions of suction and blowing, with the number of regions increasing as x_0 increases. As with V_w, because of the scalings, the physical size of W_w is very small.

B.   Flat Plate With a Pressure Gradient

Optimal perturbations in a boundary layer with a pressure gradient were considered in Ref. 1. The pressure distribution corresponded to the model designed at the NASA Glenn Research Center that was used to study the flow over a LPT blade. This case has the scalings $L_{ref} = L_s$, where L_s is the suction surface length and $U_{ref} = U_{exit}$, where U_{exit} is the nominal exit free-stream velocity based on the inviscid solution.[1,6] The optimal inflow disturbance was applied at $x_0/L_s = 0.125$ and $x_0/L_s = 0.25$ with the optimal energy growth occurring at $x/L_s = 0.5$. For each choice of x_0/L_s, four values of β were considered ($\beta = 0.3$, 0.5, 0.7 and 0.9).

We again apply the optimization technique to find the blowing and suction distributions for both the normal and tangential velocities at the wall in order to generate the same streaky structures as in the case of optimal perturbations. Figures 11 and 12 show V_w for several choices of β where $x_0/L_s = 0.125$ and 0.25 respectively. For these same values of β, Figs. 13 and 14 show W_w for $x_0/L_s = 0.125$ and 0.25 respectively.

The general behavior of the relative magnitudes of V_w and W_w for choices of x_0 and β remain consistent with that shown in Figs. 3 - 6 and Figs. 7 - 10. However, in the case of a flat plate with a pressure gradient, the first region of V_w in the flow control interval is a region of suction. This region is followed by a region of blowing, and again these regions are followed by alternating regions of suction and blowing, with the number of regions increasing as x_0 increases. Additionally, for the case of a flat plate with a pressure gradient, the first region of W_w in the flow control interval is one of blowing. As with V_w, this region is followed by alternating regions of suction and blowing.

V.   Conclusions

In this paper we used an iterative method to compute the optimal control by blowing and suction at the wall that minimizes the energy of perturbations when the initial perturbation is optimal. Due to the linear nature of the governing equations, these same distributions can be used to generate the streamwise velocity streaks that would have been generated from the optimal disturbance. The magnitude of the normal and tangential velocity perturbations that can generate the velocity streaks is very small. Therefore, unlike the case of localized generators, distributed generators may be a good candidate to generate the velocity streaks that lead to bypass transition.

American Institute of Aeronautics and Astronautics

Appendix

The matrices of Eq. (8) are given as follows:

$$\mathbf{A} = \begin{bmatrix} 1 & 0 & 0 & 0 \\ U & 0 & 0 & 0 \\ V & U & 0 & 0 \\ 0 & 0 & U & 0 \end{bmatrix}, \quad \mathbf{B}_0 = \begin{bmatrix} 0 & 0 & -\beta & 0 \\ -\beta^2 & -U_y & 0 & 0 \\ 0 & -2V_y - \beta^2 & -\beta V & 0 \\ 0 & 0 & -V_y - \beta^2 & \beta \end{bmatrix}$$

$$\mathbf{B}_1 = \begin{bmatrix} 0 & -1 & 0 & 0 \\ -V & 0 & 0 & 0 \\ 0 & -2V & 0 & -1 \\ 0 & 0 & -V & 0 \end{bmatrix}, \quad \mathbf{B}_2 = \begin{bmatrix} 0 & 0 & 0 & 0 \\ 1 & 0 & 0 & 0 \\ 0 & 1 & 0 & 0 \\ 0 & 0 & 1 & 0 \end{bmatrix}$$

References

[1]Tumin, A., and Ashpis, D., Transient Growth Theory Prediction of Optimal Placing of Passive and Active Flow Control Devices for Separation Delay in LPT Airfoils, NASA/TM-2003-212228, May 2003.

[2]Cathalifaud, P., and Luchini, P., Algebraic growth in boundary layers: optimal control by blowing and suction at the wall, *Eur. J. Mech. B/Fluids*, Vol. 19, 200, pp.469-490.

[3]Andersson, P., Berggren, M., and Henningson, D., "Optimal disturbances and bypass transition in boundary layers," *Phys. Fluids*, Vol. 11, 1999, pp.134-150.

[4]Gunzburger, M., "Inverse Design and Optimisation Methods," von Karman Institute for Fluid Dynamics, Lecture Series 1997-05, April, 1997.

[5]Luchini, P., "Reynolds-number-independent instability of the boundary layer over a flat surface: optimal perturbations," *J. Fluid Mech.*, Vol. 404, 2000, pp.289-309.

[6]Volino, R.J., "Separated Flow Transition Under Simulated Low-Pressure Turbine Airfoil Conditions: Part 1 - Mean Flow and Turbulence Statistics," *Proceedings of ASME TURBO EXPO 2002 Conference*, Paper GT-2002-30236.
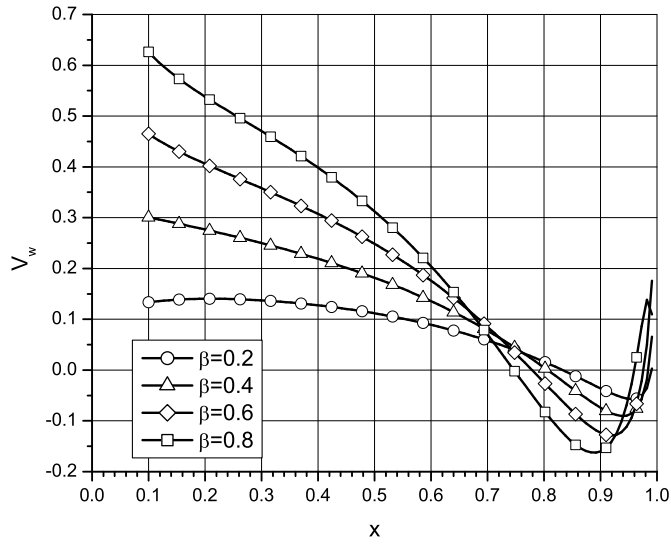
Figure 3. The blowing and suction distribution for the normal velocity at the wall for the flow control interval $[0.1, 1]$ **for four choices of** β**.**
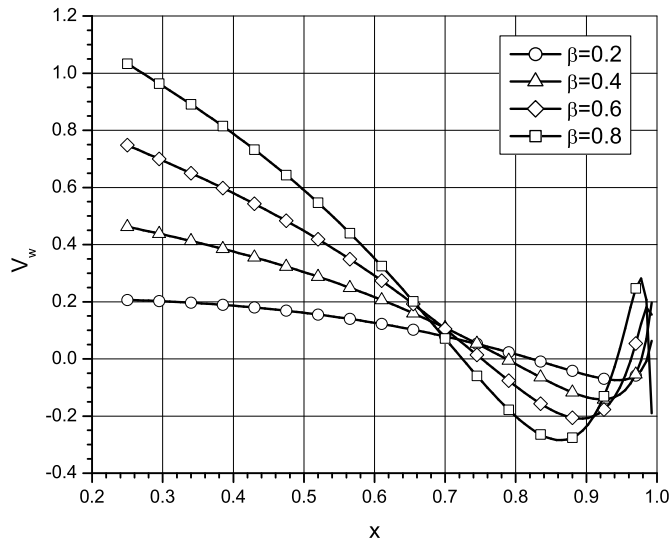

Figure 4. The blowing and suction distribution for the normal velocity at the wall for the flow control interval $[0.25, 1]$ **for four choices of** β**.**
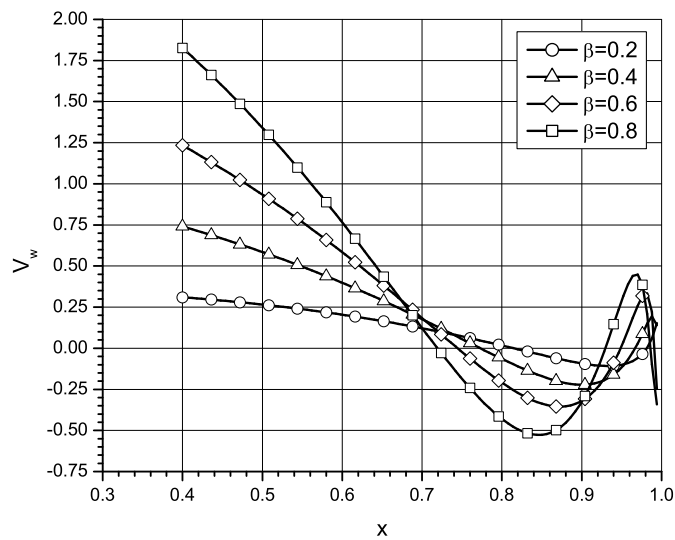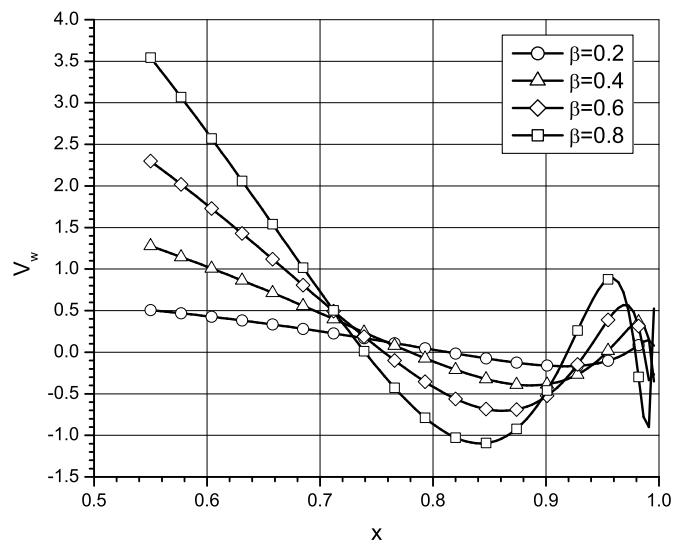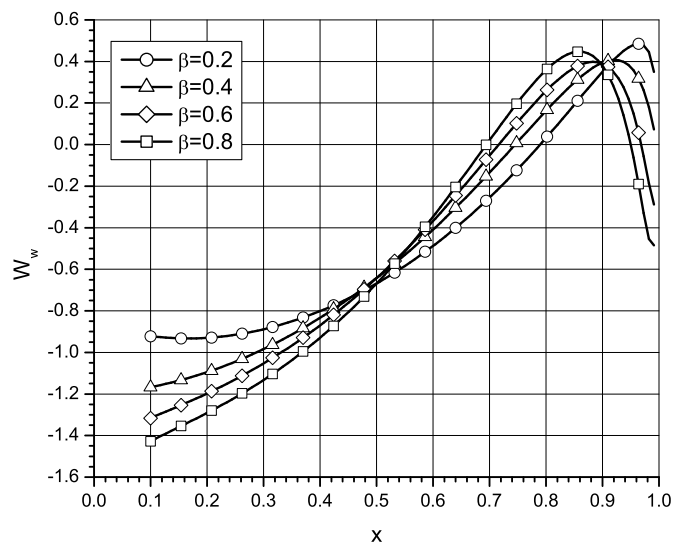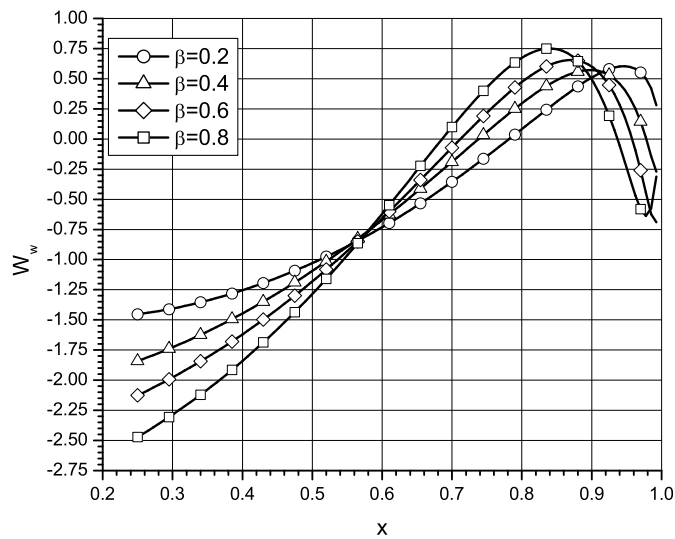
American Institute of Aeronautics and Astronautics

Figure 5. The blowing and suction distribution for the normal velocity at the wall for the flow control interval $[0.4, 1]$ **for four choices of** β**.**

Figure 6. The blowing and suction distribution for the normal velocity at the wall for the flow control interval $[0.55, 1]$ **for four choices of** β**.**

American Institute of Aeronautics and Astronautics

Figure 7. The blowing and suction distribution for the tangential velocity at the wall for the flow control interval $[0.1, 1]$ for four choices of β.

Figure 8. The blowing and suction distribution for the tangential velocity at the wall for the flow control interval $[0.25, 1]$ for four choices of β.
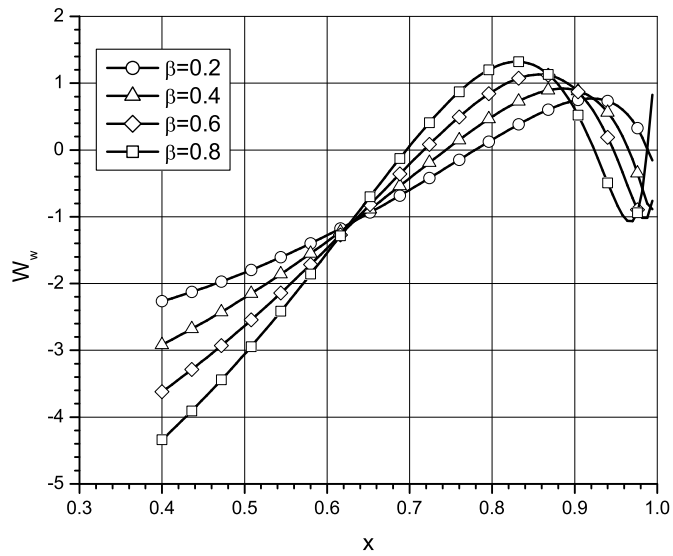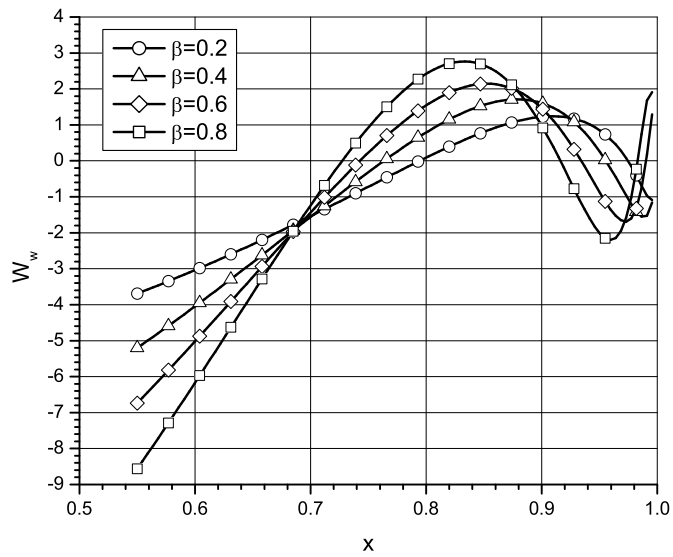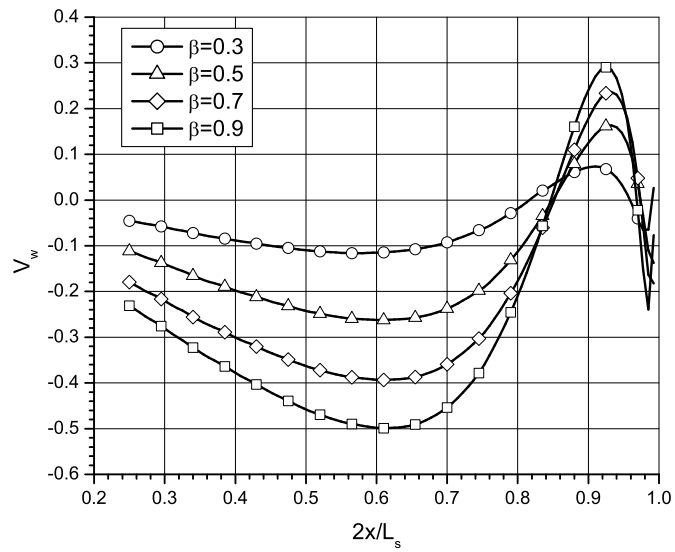
American Institute of Aeronautics and Astronautics

Figure 9. The blowing and suction distribution for the tangential velocity at the wall for the flow control interval $[0.4, 1]$ for four choices of β.

Figure 10. The blowing and suction distribution for the tangential velocity at the wall for the flow control interval $[0.55, 1]$ for four choices of β.

American Institute of Aeronautics and Astronautics

Figure 11. The blowing and suction distribution for the normal velocity at the wall for the flow control interval $[0.125, 0.5]$ **for four choices of** β.
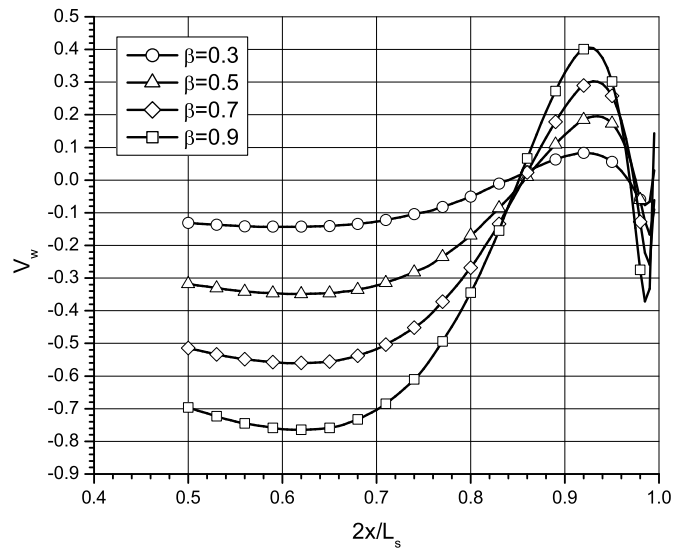

Figure 12. The blowing and suction distribution for the normal velocity at the wall for the flow control interval $[0.25, 0.5]$ **for four choices of** β.

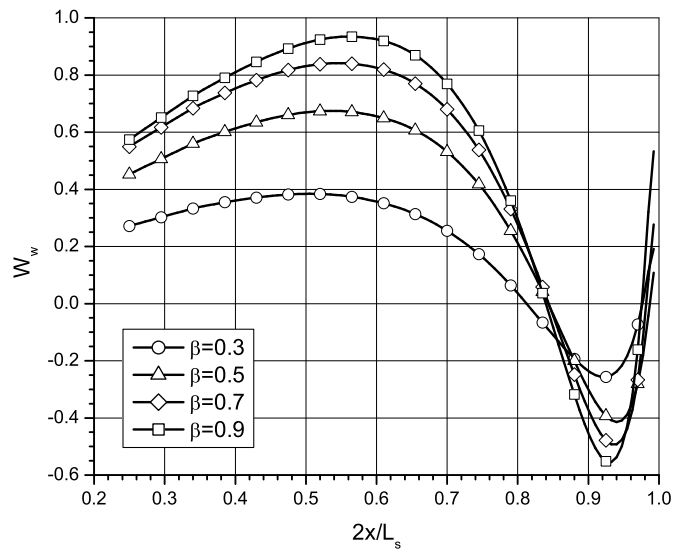American Institute of Aeronautics and Astronautics

Figure 13. The blowing and suction distribution for the tangential velocity at the wall for the flow control interval $[0.125, 0.5]$ for four choices of β.
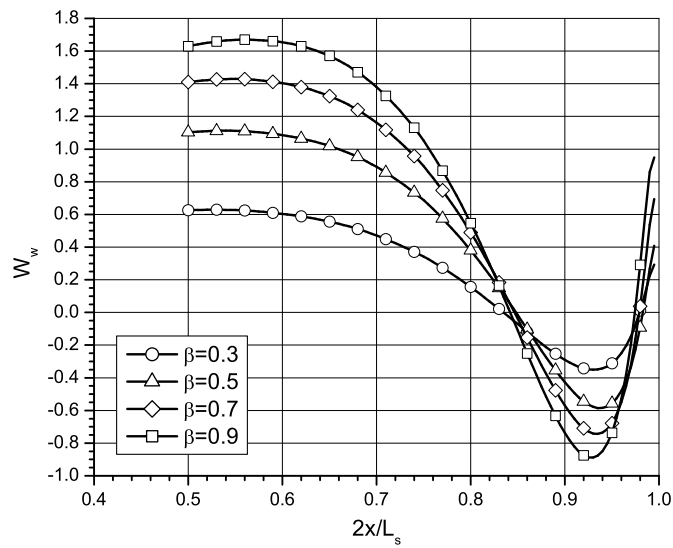

Figure 14. The blowing and suction distribution for the tangential velocity at the wall for the flow control interval $[0.25, 0.5]$ for four choices of β.

American Institute of Aeronautics and Astronautics